Dipole-on-dielectric model for infrared lithographic spiral antennas

Glenn D. Boreman

Center for Research and Education in Optics and Lasers and Department of Electrical Engineering, University of Central Florida, Orlando, Florida 32816

Aristide Dogariu

Center for Research and Education in Optics and Lasers, University of Central Florida, Orlando, Florida 32816

Christos Christodoulou

Department of Electrical Engineering, University of Central Florida, Orlando, Florida 32816

Dale Kotter

Idaho National Engineering Laboratory, Lockheed-Martin Corporation, P.O. Box 1625, Idaho Falls, Idaho 83415

Received September 7, 1995

We present a dipole-on-dielectric model for lithographic antennas used for bolometer coupling in the infrared. The predicted antenna patterns show good agreement with measurements of Au-on-Si spiral antennas at 9.5-μm wavelength. Angle- and polarization-resolved measurements are proposed, which will further probe the behavior of these antenna structures and facilitate refinement of the analytical models. © 1996 Optical Society of America

Planar lithographic antennas are widely used in the far-infrared and millimeter-wave portions of the spectrum.[1] Possible antenna configurations include dipole,[2] bow-tie,[3] log-periodic,[3] and spiral.[4] These antennas are typically illuminated through their dielectric substrates because the radiation pattern is stronger in the dielectric than in air.[5] Hemispherical lenses[1] are often placed directly in contact with the substrate to prevent angular changes in the radiation pattern that would be caused by refraction at a planar interface.

Recently, a 65° Au-on-Si spiral antenna was demonstrated[4] to facilitate coupling of 9.5-μm radiation to a subwavelength-sized uncooled bolometer. Measurements of antenna power patterns were made in two orthogonal planes with an $f/1.7$ illumination cone. The results were similar to the pattern of a 65° spiral antenna in free space.[4] This was unexpected, because a dielectric substrate significantly modifies the antenna patterns of both dipole and slot antennas compared with the patterns of free-space radiation. A complete theoretical analysis of a spiral antenna on a dielectric substrate has not, to our knowledge, been performed.[4] Our approach, a dipole antenna on a dielectric half-space, is a first step toward quantitative modeling of these structures. Our calculated antenna patterns, when convolved with an $f/1.7$ cone, agree well with the experimental data of Ref. 4.

Radiation incident upon a lithographic spiral induces propagating current waves on the antenna arms. The current waves on opposite arms will have identical directions and phases at a locus of points defined by[6–8] a circle with a circumference equal to the illumination wavelength:

$$r = \lambda/2\pi . \tag{1}$$

The constructive interference of radiation from these closely spaced phasor current sources (each of which can be individually considered a Hertzian dipole) will behave to first order, in the broadside direction, as a single dipole with an orientation parallel to the in-phase currents. Given the convolution involved in the measurements of Ref. 4, we believe that a single-dipole model will suffice until measurements are made with a collimated beam, which will allow a more detailed angular examination of the radiation patterns and subsequent refinement of the antenna model.

A spiral antenna of the type tested in Ref. 4 is shown in Fig. 1, along with a schematic of the test setup. A 0.8-μm by 2-μm Nb bolometer was fabricated on the Si substrate. Over that, a lithographically patterned Au layer comprised the antenna. The substrate was placed in contact with a Si hemispherical lens, so that radiation reached the antenna through the substrate. The bolometer resistance was monitored by a dc electrical connection to the outer portion of the antenna arms. The antenna–lens assembly was mounted in a rotation stage with a horizontal scan plane. The long axis of the bolometer was aligned either parallel or perpendicular to the electric field of a linearly polarized CO_2 laser, which was focused onto the antenna with an $f/1.7$ lens. This relatively fast $f/\#$ was used to produce

0146-9592/96/050309-03$6.00/0

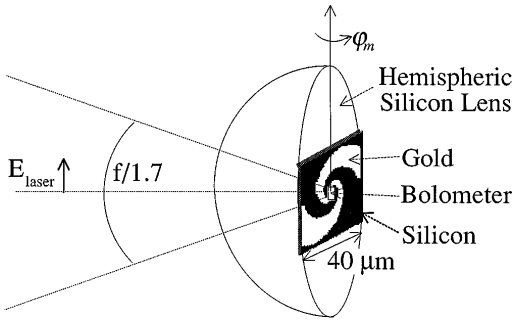

Fig. 1. Schematic of the measurement setup used in Ref. 4.

a smaller illumination spot size and an increased power density. However, the fast $f/\#$ results in a convolution of the true antenna pattern with an angular window of approximately 30°, considerably reducing the angular resolution of the measurement.

A dipole antenna at a dielectric interface[9] has the following power radiation (and, by reciprocity, the same for reception) patterns P (in watts per steradian) in the two orthogonal directions inside the dielectric:

$$P(\theta_d) = \left(\frac{\omega\mu_0 Ih}{4\pi r}\right)^2 2\sqrt{\frac{\varepsilon_0}{\mu_0}} \times n\left|\frac{n\cos[\sin^{-1}(n\sin\theta_d)]\cos\theta_d}{n\cos[\sin^{-1}(n\sin\theta_d)]+\cos\theta_d}\right|^2, \quad (2)$$

$$P(\varphi_d) = \left(\frac{\omega\mu_0 Ih}{4\pi r}\right)^2 2\sqrt{\frac{\varepsilon_0}{\mu_0}} \times n\left\{\frac{n\cos\varphi_d}{\cos[\sin^{-1}(n\sin\varphi_d)]+n\cos\varphi_d}\right\}^2, \quad (3)$$

where ω is the radian optical frequency, I is strength of the phasor current, h is the length of the current element, r is the distance from the dipole, and n is the refractive index of the dielectric, which we take as 3.4 for Si. As shown in Fig. 2, the dipole pattern is separable in θ_d and φ_d such that the radiation intensity at intermediate angles is the product of Eqs. (2) and (3).

Interpretation of the measured data from Ref. 4 must include the fact that the scans were along neither θ_d nor φ_d. The angular orientation of the equivalent dipole was a function of λ by Eq. (1), and thus the dipole was not necessarily aligned with the bolometer's long axis. We can estimate the angle α between the dipole and the bolometer's long axis. Using finite-element analysis of spiral antennas, we have found that the current sheet is not uniformly distributed across the metal arm but tends to be concentrated near the innermost surface of the arm, at a radius satisfying Eq. (1). We have not calculated the angular distribution of the surface currents in detail, but the largest currents are approximately tangent to the circle for which $r = \lambda/2\pi$. Using the equations presented in Ref. 8 for the situation in Ref. 4, that of a spiral with a 65° wrap angle and a 90° arm width, we calculate the angle β for which the radius of the inside curve of the spiral will equal $(9.5/2\pi)$ μm as

$$\exp(\beta/\tan 65°) = \frac{9.5}{2\pi}, \quad (4)$$

yielding $\beta \approx 0.89$ rad (51°). Given that the surface currents, which are parallel to the equivalent dipole direction, are tangent to this circle we set $\alpha \equiv 90° - \beta$, yielding $\alpha \approx 39°$.

Our analysis uses the two coordinate systems seen in Fig. 2. One is attached to the dipole (θ_d, φ_d), and the other is attached to the measurement apparatus (θ_m, φ_m). The two systems are related by a rotation of γ in the plane of Fig. 2. The measurement coordinate φ_m is a rotation around the long axis of the bolometer, as shown in Fig. 1. The measurements of Ref. 4 were made as a function of φ_m, for $\theta_m = 0$. Under these conditions, the coordinates are related by

$$\theta_d = \tan^{-1}\left(-\frac{\sin\varphi_m\sin\gamma}{\cos\varphi_m}\right), \quad (5)$$

$$\varphi_d = \tan^{-1}\left\{\frac{\cos\varphi_m\cos\gamma}{[(\sin\varphi_m\sin\gamma)^2+\cos^2\varphi_m]^{1/2}}\right\}, \quad (6)$$

The two orthogonal scans performed in Ref. 4 correspond to rotation angles of $\gamma = \alpha$ and $\gamma = \alpha + 90°$.

In addition to the coordinate rotation of Eqs. (5) and (6), we must project the antenna power pattern along the incident polarization vector used in Ref. 4. Substituting Eqs. (5) and (6) into Eqs. (2) and (3), we obtain expressions that are then multiplied by $\cos^2\gamma$. The resulting antenna patterns are plotted in Fig. 3 for $\gamma = 41°$ and $\gamma = 131°$ (which yield a slightly better fit to the Ref. 4 data than the predicted angles $\gamma = 39°$ and $\gamma = 129°$) as functions of φ_m. Plots are included both with and without convolution by rect$(\varphi_m/30°)$, to highlight the additional angular information that would be available if collimated radiation were used in the measurement.

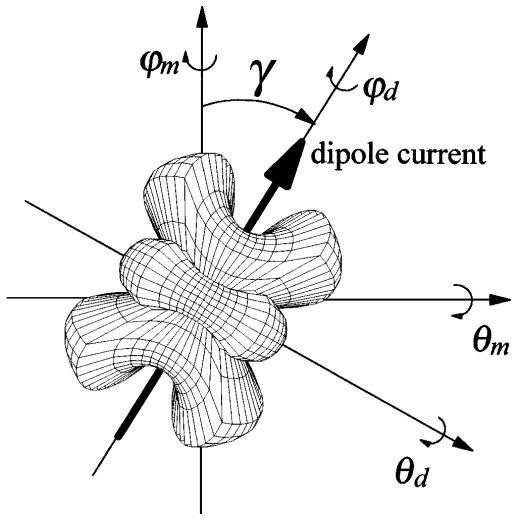

Fig. 2. Power radiation function as a function of dipole coordinates $P(\theta_d, \varphi_d)$, along with measurement coordinate system (θ_m, φ_m).

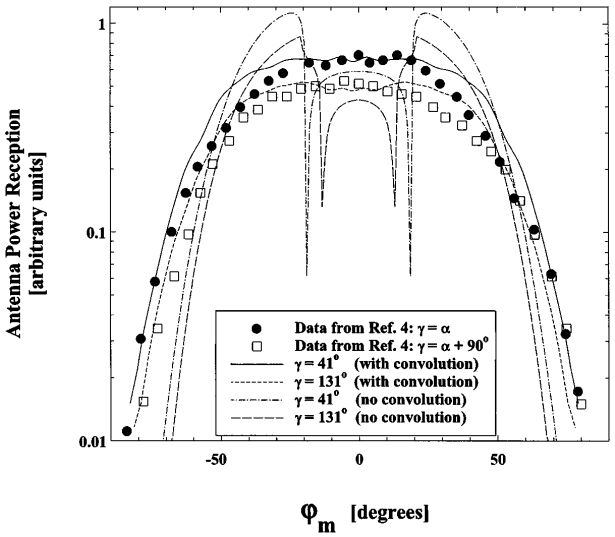

Fig. 3. Measured antenna-pattern data from Ref. 4, along with dipole-on-dielectric predictions for antenna patterns, both with and without convolution with an $f/1.7$ cone, as a function of φ_m.

Figure 3 shows that the data of Ref. 4 can be explained quite accurately by our simple model. This dipole-on-dielectric modeling approach should be useful for infrared lithographic antennas in general, because all lithographic antenna designs depend on similar spatial-resonance requirements between the wavelength and the antenna structure. In addition, the refractive index of the dielectric through which the antennas are illuminated bounds the angular width of any antenna pattern (through Snell's law) as shown by Fig. 2 and Eqs. (2) and (3).

The range of validity of this model should be explored by additional measurement of power reception patterns as functions of the in-plane rotation angle γ. Measurements should also be made with a quarter-wave plate and analyzer to determine more completely the antenna's polarization state. If these measurements are made with collimated radiation, the resulting data should permit development of more-accurate antenna models.

The next logical steps in refinement of a model for the lithographic spiral antenna would be to use a vector sum of two dipoles spaced by λ/π and then to use detailed surface-current distributions to calculate the antenna pattern resulting from a weighted sum of such dipole pairs.

This work was supported by the U. S. Department of Energy under contract C95-175599-LKK-214-95.

References

1. D. Rutledge, D. Neikirk, and D. Kasilingham, in *Infrared and Millimeter Waves,* K. J. Button, ed. (Academic, New York, 1983), Vol. 10, pp. 1–90.
2. C. Karadi, J. Jauhar, L. Kouwenhoven, K. Wald, P. McEuen, Y. Nagamune, and H. Sakaki, J. Opt. Soc. Am. B **11,** 2566 (1994).
3. R. Compton, R. McPhedran, Z. Popovic, G. Rebeiz, P. Tong, and D. Rutledge, IEEE Trans. Antennas Propag. **35,** 622 (1987).
4. E. Grossman, J. Sauvageau, and D. McDonald, Appl. Phys. Lett. **59,** 3225 (1991).
5. C. Brewitt-Taylor, D. Gunton, and H. Rees, Electron. Lett. **17,** 729 (1981).
6. H. Nakano, *Helical and Spiral Antennas* (Wiley, New York, 1987), p. 111.
7. J. Kaiser, IRE Trans. Antennas Propag. **8,** 312 (1960).
8. J. Dyson, IRE Trans. Antennas Propag. **7,** 181 (1959).
9. D. Rutledge and M. Muha, IEEE Trans. Antennas Propag. **30,** 535 (1982).